Oxygenic-hole centres in x-irradiated zircon: 10 K EPR studies

# Oxygenic-hole centres in x-irradiated zircon: 10 K EPR studies

R F C Claridge, N S Lees, W C Tennant and C J Walsby

Department of Chemistry, University of Canterbury, Private Bag 4800, Christchurch,
New Zealand

**Abstract.**    A surprisingly large number of paramagnetic hole centres in zircon have been observed and characterized by EPR. The field is reviewed and a model proposed based on some ten precisely measured centres. EPR data suggest that the trapped hole, produced by x-irradiation, is normally located in the non-bonding $p_z$ orbital of an $O^-$ ion and is stabilized by a nearby impurity cation, often, but not always, a +3 ion. Two previously unobserved oxygenic-hole centres are here reported. In one the stabilizing ion is shown from observed $^{89}Y$ superhyperfine structure to be $Y^{3+}$ and conforms to the above model. The second has the most anisotropic $g$ values yet observed in an oxygenic-hole centre in zircon. Two $g$ values are significantly below the free-electron value and a $p_x$ ground state is inferred.

## 1. Introduction

Zircon (zirconium silicate) serves as a good example of a mixed ionic–covalent crystal. Covalent $SiO_4^{4-}$ units are 'bonded' electrovalently by $Zr^{4+}$ ions, the crystal space group being tetragonal $I4_1/amd$. The electronic properties of the crystal may be influenced by impurity ions, vacancies and radiation-induced centres often at very low concentrations. Many of these centres are paramagnetic and thus amenable to study by electron paramagnetic resonance (EPR). Many EPR studies of paramagnetic defect centres (transition ions, radicals, holes and colour centres) have been reported in zircon (see [1], [2] and references therein). The EPR spectra of most centres studied reflect one of two point-group symmetries: $\bar{4}2m$ ($D_{2d}$), Laue class $4/mmm$ ($D_{4h}$) uniaxial (tetragonal), for ions substituting in the Zr or Si lattice positions (Wyckoff [3] letter a or b), or point-group symmetry $m$ ($C_S$), Laue class $2/m$ ($C_{2h}$), for centres on or interacting with ligand oxygens (Wyckoff positions h) lying in the $ac$ or $bc$ mirror planes. Occasionally centres with point-group symmetry 2, i.e. lying on one of the dihedral twofold axes, have been observed (e.g. P centre [4]). Barker and Hutton [5] have also reported a hole centre, stabilized by a nearby Y atom, where the site symmetry is lowered to $\bar{1}$ ($C_i$).

Considering that there is but one type of O atom in the ideal zircon lattice, EPR studies of oxygenic-hole centres in zircon form a surprisingly complex field as is well illustrated in the review article by Krasnobaev *et al* [1]. Figure 1(a) has been adapted and expanded from this reference. From figure 1(a) the anisotropy in the observed $g$ values is seen to vary from nearly isotropic (No 1) to highly anisotropic (No 29). The corresponding orbital splittings, obtainable from a crystal-field analysis of the principal $g$ values, cover a range from a few thousand $cm^{-1}$ to almost complete orbital quenching in No 1 [6, 7]. The hole centres studied
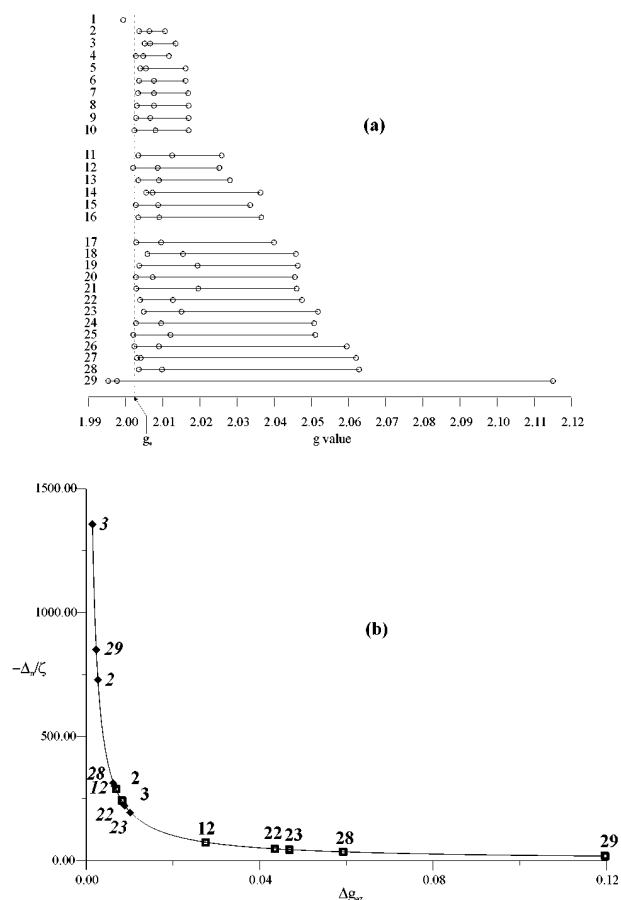
**Figure 1.** (a) Anisotropy in $g$ values of hole centres in zircon (adapted from [1]): 1, C centre [6, 7]; 2, D centre [2]; 3, RT centre [2]; 4, $SiO_2^{3-}$ [1]; 5, $SiO_2^{3-}/OH^-$ [1]; 6, $SiO_4^{3-}/Y^{3+}$ [5]; 7, $SiO_4^{3-}/Y^{3+}$ [24]; 8, $SiO_2^{3-}/2Y^{3+}$ [1]; 9, $SiO_2^{3-}/Y^{3+}$ [1]; 10, $[SiO_3-SiO_4]^{5-}-2Y^{3+}$ [25]; 11, $SiO_3^-/Y^+$ [1]; 12, $SiO_4^{3-}/Y^{3+}$ [15]; 13, $AlO_3^{2-}$ [1]; 14, $SiO_3^-/H^+$ [1], 15, $SiO_3^-/2H^+$ [1]; 16, $SiO_3^-/V(Zr)$ [1]; 17, $SiO_4^{3-}/OH^-$ [1]; 18, $AsO_4^{2-}$ [1]; 19, $SiO_4^{3-}/2H^+$ [1]; 20, $SiO_4^{3-}/(H_2O + V(Zr))$ [1]; 21, $SiO_4^{3-}/(H_2O+V(Zr)+V(O))$ [1]; 22, $[BO_4]^0$ [8]; 23, $[AlO_4]^0$ [9]; 24, $[AlO_4]^{4-}$ [1]; 25, $[AlO_4]^{4-}$ [25]; 26, $SiO_4^{3-}/Y^{3+}$ [1]; 27, $SiO_4^{3-}$ [25]; 28, $[SiO_4/Y]^0$ [this work]; 29, $[SiO_4/M]^0$ [this work]. (Note, in general the nomenclature of [1] has been retained). (b) Plot of dimensionless orbital splitting versus $\Delta g$ for a selection of hole centres in zircon: ♦ $= \Delta_1/\zeta$ versus $(g_y - g_z)$ and □ $= \Delta_2/\zeta$ versus $(g_x - g_z)$ (refer to text and appendix); $\zeta$ is the spin–orbit coupling constant. The numbering of centres is as for figure 1(a).

in this laboratory, the C centre, No 1 [6, 7], the D and RT centres, Nos 2, 3 [2], the $[BO_4]^0$ centre, No 22 [8], the $[AlO_4]^0$ centre, No 23 [9] and the two centres which are the subject of this paper (Nos 28, 29), cover the whole range of $g$ anisotropies from the smallest to the largest. Allowing that a few of the centres summarized in figure 1(a) may be the same centre with small experimental differences in determined $g$ values (e.g. Nos 23, 24, 25 are all reported as Al-stabilized hole centres and may well all be the same centre), there remain at least ten well characterized oxygenic-hole centres and probably twice as many again tentative reports (see again [1]).

The probable mechanism of formation of the oxygenic-hole centres can be inferred by reference to studies of similar centres in $\alpha$-SiO$_2$ [10, 11], GeO$_2$ [12, 13] and $\beta$-Al$_2$O$_3$ [14]. The hole is thought to be trapped in a p orbital of an O$^-$ ion (leaving an electron with unpaired spin in this orbital) and stabilized by an impurity cation located in one of the Si or Zr lattice positions. The basic unit can therefore be envisaged as SiO$_4^{3-}$ leading to the designation [SiO$_4^{3-}$/M$^{3+}$]$^0$ (or simply [SiO$_4$/M]$^0$) when a stabilizing +3 ion is present in a nearest-neighbour Si or Zr lattice position. This cation evidently enhances the stability of the centre if it is of lower positive valence than that of Zr$^{4+}$; Al$^{3+}$ [9], B$^{3+}$ [8] and Y$^{3+}$ [5, 15] (and the [SiO$_4$/Y]$^0$ centre of this paper) are examples of +3 cations which have been observed. A more extreme example of this trapping mechanism is that of the so-called C centre [6] which has been re-interpreted recently [7] as an oxygenic electron–hole centre stabilized by an adjacent Zr$^{4+}$ vacancy; in this case the centre is particularly stable, i.e. the hole can be said to be in a very 'deep' trap.

Thus the multitude of oxygenic-hole centres observed in zircon can be understood qualitatively as being due to various stabilizing +3 (or perhaps lower valence) ions in nearest-neighbour Si or Zr sites. In a few cases the nature of the stabilizing ion can be inferred from observed hyperfine structure (hfs), e.g. Al$^{3+}$ ($^{27}$Al, $I = 5/2$, 100% abundant), Y$^{3+}$ ($^{89}$Y, $I = 1/2$, 100%) and B$^{3+}$($^{10}$B, $I = 3$, 19.8%; $^{11}$B, $I = 3/2$, 80.2%). It is noted that hfs is not always observed making identification of the stabilizing ion difficult.

Following the arguments of Stapelbroek *et al* [12] one might have expected the hole to be located in a p orbital oriented along an O$^-$–M$^{3+}$ direction. However an analysis of the $g$ values of the centres of figure 1(a) indicates that in almost all cases reported for zircon the hole is located in the non-bonding p$_z$ orbital directed perpendicular to the mirror plane containing the O$^-$ ion. Analysis of the $g$ values of some of the reported hole centres leads to the orbital splittings plotted in figure 1(b)—the extreme case is that of the C centre [7]. Note that we have only analysed the $g$ values, and plotted results in figure 1(b) for the hole centres studied in this laboratory and one other [15] for which, in each case, the $g$ parameter matrix was well determined. The dimensionless orbital splittings for the C centre, $\Delta_1/\zeta$ and $\Delta_2/\zeta$, are 15 375 and 100 393 respectively and are well outside the vertical scale of figure 1(b) and are not plotted in figure 1(b).

In this paper we report detailed studies of two further oxygenic-hole centres formed when a synthetic zircon crystal deliberately doped with small amounts of TiO$_2$ and Y$_2$O$_3$ was irradiated with x-rays at 77 K, transferred cold to the EPR cavity and the temperature reduced to ~15 K for EPR measurements.

One of the centres, sometimes hereafter referred to as the 'split' centre (No 28, figure 1), exhibits super-hfs from a nearby 100% abundant $I = 1/2$ nucleus thought to be $^{89}$Y. (This centre may be the same as Nos 26, 27 of figure 1 but has not hitherto been analysed with the precision herein reported.) The second centre, herein often referred to as the 'unsplit' centre (No 29 of figure 1), has no obvious hfs for identification; it does not appear to be one of those previously studied.

In some respects the spectra of the two hole centres are similar: each has point-group symmetry $m$ (C$_S$) and their spectra are coincident when the crystal is aligned with the crystallographic $c$ axis parallel to the static magnetic field. The split centre appears typical of hole centres where the hole is trapped in the non-bonding p$_z$ orbital of the O$^-$ ion. The unsplit centre however is different in two respects from most other centres (see figure 1(a)): the $g$ anisotropy is greater than for any other oxygenic-hole centre so far reported in zircon and two of the $g$ values are significantly lower than the free-electron value. We believe in this case that the hole is trapped in a p$_x$ (or p$_y$) orbital directed in the crystal mirror plane.
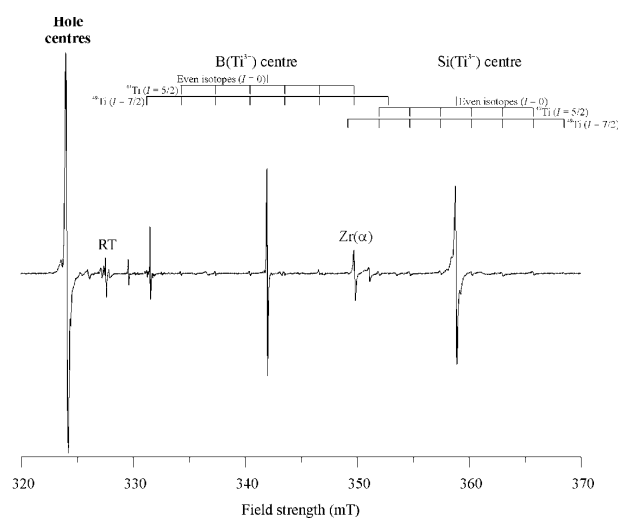
## 2. Experiment

The zircon crystals were grown from a melt containing $Li_2SiO_3$–$ZrO_2$ in a flux of $Li_2MoO_4$–$MoO_3$ (with added 0.1% molar $TiO_2$ and $Y_2O_3$) [16] and is the same as the one in which the recently reported $Si(Ti^{3+})$ centre [4] was contained. The crystal had natural faces parallel to the *ac* and *bc* planes which allowed precise alignments, $\pm 2$ minutes of arc, for the experimental measurements. Measurements were made in 5–10° intervals in the *bc* plane. The magnetic field was measured with a Bruker Gaussmeter to $\pm 0.002$ mT and the microwave frequency with a Systron Donner counter to $\pm 1$ kHz.

## 3. Results

The spectrum of both centres with the static magnetic magnetic field parallel to the crystallographic *c* axis consisted of a single, rather broad, intense line. The hfs on the split line was partially obscured in this orientation by the broader unsplit centre. The peak-to-peak linewidths are 0.18 mT for the unsplit centre and 0.06 mT for the split centre. The positions of the two hole centres are shown in relation to a previously reported hole centre RT [2] and to the titanium centres $B(Ti^{3+})$ [17] and $Si(Ti^{3+})$ [4] in the *c*-axis spectrum of figure 2. The angular dependences of the two centres in the *bc* plane are depicted in figure 3. Along the *c* axis the centres are seen to be almost coincident. Alignment of the crystal was confirmed by observing the $Zr(\alpha)$ [2] centre which is known, from earlier experiments, to collapse from three symmetry-related sites in the *bc* plane to one when the crystal *c* axis is parallel to the static field. Both centres were irreversibly destroyed on warming the crystal to room temperature. This mirrors the behaviour of the previously reported D centre but contrasts with that of the so-called RT centre [2] which, as the name implies, persists after the crystal is warmed to room temperature; this centre in fact, as apparently distinct from all previously reported hole centres, is observable by EPR at room temperature and must be a very stable centre.

The spectra from the two centres were fitted to the spin Hamiltonian (SH)

$$\aleph_S = \beta_e \boldsymbol{S} \cdot \bar{g}_i \cdot \boldsymbol{B} + [\boldsymbol{S} \cdot \bar{A}_i \cdot \boldsymbol{I} - \beta_n \boldsymbol{I} \cdot (\bar{g}_n)_i \cdot \boldsymbol{B}] \tag{1}$$



**Figure 2.** *c*-axis spectrum of the $[SiO_4/Y]^0$ and $[SiO_4/M]^0$ centres in relation to other designated centres; $\nu = 9.2195$ GHz, $T = 15$ K.
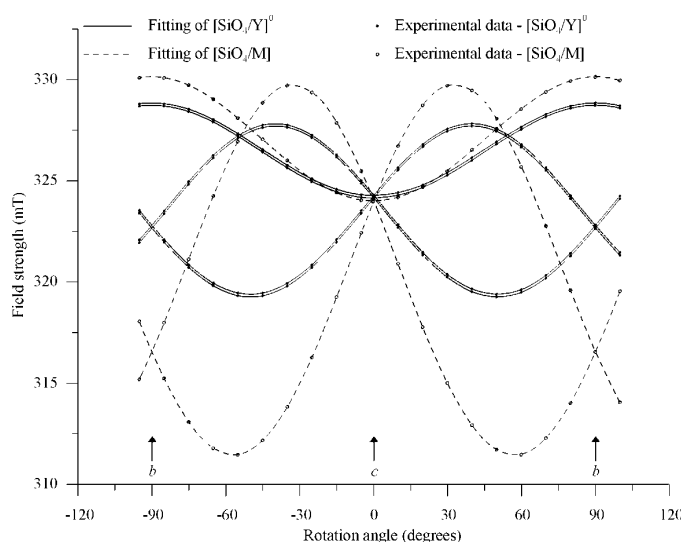
**Figure 3.** Angular dependence of the $[SiO_4/Y]^0$ and $[SiO_4/M]^0$ centres in the $bc$ plane of the crystal.

**Table 1.** Spin-Hamiltonian parameters for the $[SiO_4/M]^0$ and $[SiO_4/Y]^0$ centres in zircon. $[SiO_4/M]^0$: number of data points = 84, number of unit-weighted data points = 72, RMSD = 0.009 mT. $[SiO_4/Y]^0$: number of data points = 168, number of unit-weighted data points = 124, RMSD = 0.006 mT.

| | Matrix $\bar{Y}$ | | | $k$ | Principal value, $Y_k$ | Principal directions $\theta_k$ (°) | $\phi_k$ (°) |
|---|---|---|---|---|---|---|---|
| $[SiO_4/M]^0$ | | | | | | | |
| | 2.080 26(1) | 0 | 0.053 56(1) | 1 | 2.114 97(2) | 57.05(0) | 0 |
| $\bar{g}$ | | 1.995 27(1) | 0 | 2 | 1.997 62(2) | 147.05(0) | 0 |
| | | | 2.0323 39(1) | 3 | 1.995 27(1) | 90 | 270 |
| $[SiO_4/Y]^0$ | | | | | | | |
| | 2.040 952(6) | 0 | 0.0261 29(6) | 1 | 2.062 809(7) | 50.09(0) | 0 |
| $\bar{g}$ | | 2.003 487(6) | 0 | 2 | 2.009 716(7) | 140.09(0) | 90 |
| | | | 2.031 574(6) | 3 | 2.003 487(6) | 90 | 90 |
| | 0.139(2) | 0 | 0.010(2) | 1 | 0.144(2) | 61.3(8) | 0 |
| $\bar{A}/g_e\beta_e$ | | 0.117(2) | 0 | 2 | 0.120(2) | 151.3(8) | 0 |
| ($^{89}$Y) (mT) | | | 0.126(2) | 3 | 0.117(2) | 90 | 90 |

where the terms in the square brackets refer only to the $^{89}$Y split centre and the subscripts refer to the $i = 1$–4 symmetry-related sites of the $C_4$ rotation group which is appropriate for sites of $2/m$ Laue class (point group symmetries 2, $m$ or $2/m$) in a tetragonal crystal; it is noted however that the full rotation group is $D_4$ [18]. The nuclear $g_n$ matrix for $^{89}$Y was taken as the isotropic matrix $-0.274\,835\,\mathbf{U}$ where $\mathbf{U}$ is the $3 \times 3$ unit matrix. Data for both centres were fitted with programme EPRNMR [19] and resulted in the parameter matrices shown in table 1. In both cases the fit obtained was within the inherent scatter in the data (root-mean-squared deviation (RMSD) $\leqslant$ (peak-to-peak linewidth)/3).

## 4. Discussion

In the following discussion we shall consider it established that the oxygenic-hole centres subject of this paper result from trapping of an electron–hole in a ligand oxygen p orbital as a result of x-irradiation. The discussion is based particularly upon EPR studies of the two 'new' centres herein described, the D and RT centres described in [2], the two Y-stabilized centres studied by Hutton and co-workers [5, 15], and the centres $[BO_4]^0$ [8] and $[AlO_4]^0$ [9]. Various other hole centres reported in the literature (see [1]) may form in the same way but, in the absence of detailed single crystal studies, the data are less definitive. We have seen no evidence for oxygen-vacancy centres in the hole centres studied in this laboratory. For example, one might expect to observe, in addition to an electron-vacancy centre, F-centre-type defects where an unpaired electron occupies the oxygen vacancy. Such centres are characterized by approximately isotropic $g$ values near 2.0023. It is noted however that it has been claimed that oxygen-vacancy hole centres based on $SiO_2^{3-}$ and $SiO_3^-$ units have been observed by EPR (see particularly [1]).

It is appropriate at this stage to consider in more detail the crystal-field analysis of the observed $g$ values for the two new centres here reported. We essentially follow the treatments outlined by Vannotti and Morton [20] and Stapelbroek *et al* [12], except that we shall use numerical diagonalizations of the energy matrices involved. For a site of point-group symmetry $m$ the $p_x$ and $p_y$ orbitals transform as bases for the $A'$ irreducible representation while $p_z$ transforms as the $A''$ representation. The orbital levels are mixed by the spin–orbit coupling interaction which can be written generally $\zeta \Sigma_i k_i l_i \cdot s_i$ (where $k_i$ ($i = x, y, z$) are the orbital reduction factors). Possible ground configurations are $1s^2 2s^2 2p_x^2 2p_y^2 2p_z^1$ and $1s^2 2s^2 2p_x^1 2p_y^2 2p_z^2$ (i.e. either $p_z$ or $p_x$ (or $p_y$) as ground state); both are considered. The complex $6 \times 6$ matrix of the crystal field spin–orbit coupling Hamiltonian block diagonalizes into two $3 \times 3$ matrices, numerical diagonalization of which produces three Kramers' doublets and their corresponding eigenvectors. The $g$ values in the ground state are calculated from the eigenvectors and the magnetic field Hamiltonian $\aleph_{Zeeman} = \beta_e (l + \alpha g_e s) \cdot B$ where the empirical factor $\alpha$ allows the ground-state $g$ value to differ from the free-electron value either through delocalization, spin polarization or covalency effects. If $p_x$ (or $p_y$) is the ground state, two of the $g$ values may be less than the free-electron value (see also appendix). The ground-state $g$ value with $p_z$ lowest usually considerably exceeds the free-electron value. In the present studies we shall see below that $p_z$ as ground state covers most of the hole centres observed in zircon—the hole is evidently trapped in non-bonding $p_z$ lobes directed perpendicular to the mirror plane containing the ligand O atoms. When $p_x$ is chosen as the ground state the hole is trapped in the plane of the ligand Os and the corresponding $g$ value directed towards, or approximately towards, the stabilizing cation.

In each of the above cases the observed $g$ values were least-squares fitted to the calculated $g$s by iteratively stepping the orbital splittings. Because orbital reduction factors were not known and not obtainable from the EPR experiments, it was found convenient to obtain the orbital splittings as dimensionless quantities $\Delta_1/\zeta$, $\Delta_2/\zeta$, $\delta_1/\zeta$, and $\delta_2/\zeta$, where $\Delta_1 = E_{p_x} - E_{p_z}$, $\Delta_2 = E_{p_y} - E_{p_z}$, $\delta_1 = E_{p_z} - E_{p_x}$, $\delta_2 = E_{p_y} - E_{p_x}$ and $\zeta$ is the spin–orbit coupling constant. The results are listed in table 2. The dimensioned orbital splittings of table 2 are based on $-135$ cm$^{-1}$ for the O$^-$ free ion spin–orbit coupling constant obtained from extrapolation of an isoelectronic sequence of ions [12, 21]. In both cases a $g$ fit in agreement to within experimental error is obtained. The ground-state p wavefunctions obtained are:

$$|\Psi_\pm\rangle = 0.999\,89|p_z\rangle \mp 0.001\,58|p_x\rangle - i0.014\,64|p_y\rangle \qquad \alpha = 1.000\,571$$

**Table 2.** Orbital splittings obtained for the two hole centres under study[a].

| $[SiO_4/Y]^0$ | ('split') | $[SiO_4/M]^0$ | ('unsplit') |
|---|---|---|---|
| $-\Delta_1/\zeta$ | 312.17 | $-\delta_1/\zeta$ | 849.19 |
| $-\Delta_2/\zeta$ | 34.09 | $-\delta_2/\zeta$ | 17.48 |
| $\Delta_1$ | 42 143 cm$^{-1}$ | $\delta_1$ | 114 641 cm$^{-1}$ |
| $\Delta_2$ | 4602 cm$^{-1}$ | $\delta_2$ | 2360 cm$^{-1}$ |

[a] The dimensioned orbital splittings are based on $\zeta = -135$ cm$^{-1}$ for the O$^-$ free-ion spin-orbit coupling constant.

and

$$|\Psi_{\pm}\rangle = 0.999\,59|p_x\rangle \mp i0.001\,57|p_y\rangle \mp 0.028\,55|p_z\rangle \qquad \alpha = 0.999\,250$$

respectively for the $[SiO_4/Y]^0$ and $[SiO_4/M]^0$ centres.

This rather crude analysis neglects any s-orbital mixing arising from an excited-state $1s^2 2s^1 2p^6$ configuration (see [13]). The empirical factor $\alpha$ may be regarded as an indication of the extent of delocalization of the unpaired electron to, for example Y$^{3+}$, and/or s–p hybridization of the O orbitals involved. In either case the effect is to make the centre more 'hole-like' in character. In the unsplit $[SiO_4/M]^0$ centre on the other hand $\alpha = 0.999\,25$ indicating perhaps mixing of the predominantly p-type ground-state wavefunction with the trapped electron in the adjacent M cation orbitals, the centre then becoming less 'hole-like'. (The fit is almost as good, and the wavefunctions little different from above if one takes $\alpha = 1$.)

We are now in a position to consider and comment upon the orientation of the $g$ and $A$ parameter matrices in the unit cell. The $[SiO_4/Y]^0$, split, centre is discussed first. As demanded by crystal symmetry, one principal direction of all interaction matrices with Laue class $2/m$ must lie perpendicular to the plane containing the ligand O and the Y atoms. As seen from table 1, and as discussed above, this is the direction of the $p_z$ orbital lobes containing the trapped hole and its associated unpaired electron. There is no symmetry requirement for the remaining two $g$-matrix principal directions to have any particular relationship to specific bond directions. However the largest magnitude $g$ value, $g_1$ from table 1, lies just 1.6° away from the direction from the oxygen hole to a nearest-neighbour Si while $g_2$ lies 6.5° away from the direction to a nearest-neighbour Zr. (These calculations refer to the ideal lattice positions and take no account of distortions which may occur when foreign ions are introduced.) The largest magnitude $^{89}$Y hf value, $A_1$ of table 1, lies 3.7° away from the same Zr–O direction.

For the unsplit $[SiO_4/M]^0$ centre no resolved super hfs was observed. The $g$ value apparently corresponding to the hole orbital, $g_2$ of table 1, lies almost exactly along an O–nearest-neighbour Zr direction. $g_3$ lies parallel to $b$ as demanded by symmetry. The fact that some principal directions lie almost along an O–Si direction may be coincidental—the Si–O–Zr angle is 100°. When a stabilizing cation replaces Si in the lattice however, it is the O–Si direction which coincides approximately with a principal value of the $g$ and $A$ parameter matrices, as for example in the $[AlO_4]^0$ [9] and $[BO_4]^0$ [8] centres.

The proposition that the electron–hole and its associated unpaired electron reside almost entirely in a p orbital of the ligand O means that one expects only very small superhyperfine splittings from a nearby stabilizing cation. Only when there is signature hfs from a 100% abundant nucleus can one obtain reliably a hyperfine interaction matrix. If one utilizes the observed superhyperfine matrices and the tables of Morton and Preston [22] the following spin densities are obtained on the stabilizing ions: $[SiO_4/Y]^0$ 1.5% (this paper), $[AlO_4]^0$ 2.08% [8, 9] and $[BO_4]^0$ 5.04% [8]. That is, some 95–99% of the spin density is associated apparently with the p orbitals of O$^-$. Observation of $^{17}$O super-hfs would be needed to

verify this experimentally but the natural abundance (0.038%) of the $^{17}$O isotope ($I = 5/2$) was too small to allow this in any of our experiments with hole centres in zircon. That such measurements are feasible in crystalline solids is nicely illustrated in the paper of Nuttall and Weil [11] reporting on the $[AlO_4]^0$ centre in $\alpha$-quartz.

In the case of the unsplit $[SiO_4/M]^0$ centre where there is no resolved super-hfs we can only speculate on the identity of the stabilizing cation. One distinct possibility is Ti, presumably as $Ti^{4+}$, one of the impurity ions added to the flux mixture during crystal preparation. In this case the nuclear spins and abundances are $^{47}$Ti, $I = 5/2$, 7.4% and $^{49}$Ti $I = 7/2$, 5.4%. Even in the event that the outer hyperfine components of the 7/2 isotope were resolved, the intensity would be only around 0.5% of that of the main line and therefore probably not detectable. One cannot exclude the possibility that a lower-valence cation such as $Ca^{2+}$ or $Mg^{2+}$ may be involved. In either case the same arguments as above apply but, in addition, the greater ionic radius may, through local distortion and perhaps strain broadening, lead to the observed larger linewidth [23]. We have noted earlier that the linewidth of the unsplit $[SiO_4/M]^0$ centre is fairly broad at around 0.18 mT peak-to-peak (about three times that of the $[SiO_4/Y]^0$ centre).

In summary, we believe that the two 'new' electron–hole centres discussed in this paper are described adequately by a model in which the hole is trapped together with an unpaired electron in a p orbital of a ligand O with point-group symmetry $m$ and stabilized in each case by a nearby cation, valence +3 in the case of the $[SiO_4/Y]^0$ centre. The relatively large number of hole centres found in x-irradiated zircon, most with very similar principal directions for their interaction matrices, are explained in terms of different stabilizing cations either in the Zr or Si positions in the lattice. The stabilizing cations so far identified, via their super-hfs, have been +3 valence state, e.g. $Al^{3+}$, $B^{3+}$ and $Y^{3+}$. One could speculate that a lower-valence-state cation, $Mg^{2+}$ or $Ca^{2+}$ might lead to a more stable, more deeply trapped hole. For example the room-temperature-stable hole centre (RT, No 3 of figure 1) reported by Claridge *et al* [2], where no stabilizing cation was identified, may be such an example. We have noted the extreme case in respect of the so-called C centre [6, 7] now known to be an electron–hole centre trapped on a ligand O together with an adjacent $Zr^{4+}$ vacancy.

Finally, one could speculate that in the absence of any foreign stabilizing cation, or perhaps with a substitutional +4 cation such as $Ti^{4+}$, the hole centre may be stabilized by adopting a lower-energy electronic state, namely with the hole trapped in a p orbital directed towards $Ti^{4+}$. Is this the explanation for formation of our unsplit centre, whose $g$ values indicate a different electronic ground state from any other of the plethora of oxygenic-hole centres thus far observed in zircon?

## Acknowledgment

## Appendix

The following outlines a perturbation treatment equivalent to the numerical analysis of the $g$ values as outlined in the text. The orbital splittings and energy levels are as defined in the previous section. The eigenvalues and eigenvectors of the crystal-field spin–orbit Hamiltonian matrix are obtained to second-order perturbation and the $g$ values in the ground state obtained from the magnetic field interaction $\aleph_{Zeeman} = \beta_e[l + g_e s]\cdot B$. The $g$ values to second order are:

(i) $|p_z\rangle \sim |A''\rangle$ ground state

$$g_x = g_e \left\{ N_1^2 - \frac{2N_1\zeta}{g_e\Delta_2} - \frac{\zeta^2}{4\Delta_1^2} + \frac{\zeta^2}{4\Delta_2^2} \right\}$$

$$g_y = g_e \left\{ N_1^2 - \frac{2N_1\zeta}{g_e\Delta_1} + \frac{\zeta^2}{4\Delta_1^2} - \frac{\zeta^2}{4\Delta_2^2} \right\}$$

$$g_z = g_e \left\{ N_1^2 - \frac{\zeta^2}{4\Delta_1^2} - \frac{\zeta^2}{4\Delta_2^2} + \frac{\zeta^2}{g_e\Delta_1\Delta_2} \right\}$$

where

$$N_1^2 = \left\{ 1 - \frac{\zeta^2}{4\Delta_1^2} - \frac{\zeta^2}{4\Delta_2^2} \right\}$$

(ii) $|p_x \sim |A'\rangle$ ground state

$$g_x = g_e \left\{ N_2^2 - \frac{\zeta^2}{4g_e\delta_1\delta_2} - \frac{\zeta^2}{4\delta_1^2} - \frac{\zeta^2}{4\delta_2^2} \right\}$$

$$g_y = g_e \left\{ N_2^2 - \frac{2N_2\zeta}{g_e\delta_2} - \frac{\zeta^2}{4\delta_1^2} + \frac{\zeta^2}{4\delta_2^2} \right\}$$

$$g_z = g_e \left\{ N_2^2 - \frac{2N_2\zeta}{g_e\delta_1} + \frac{\zeta^2}{4\delta_1^2} - \frac{\zeta^2}{4\delta_2^2} \right\}$$

where

$$N_2^2 = \left\{ 1 - \frac{\zeta^2}{4\Delta_1^2} - \frac{\zeta^2}{4\Delta_2^2} \right\}.$$

Using the dimensionless orbital splittings indicated in table 2 the perturbation $g$ values calculated from the above formulae are:

(i) $[SiO_4/Y]^0$ $g_x = 2.0625$, $g_y = 2.0094$, $g_z = 2.0030$,
(ii) $[SiO_4/M]^0$ $g_x = 1.9960$, $g_y = 2.1135$, $g_z = 1.9983$

in fairly good agreement with the experimental $g$ values (table 1) and those obtained by matrix diagonalization. From (i) above, to first order, $g_x - g_z = -2\zeta/\Delta_2$ and $g_y - g_z = -2\zeta/\Delta_1$. One expects then a linear relationship in the plots $\Delta g_\alpha$ against $1/\Delta_i$ ($\alpha = x$, $y$: $i = 1, 2$) with slope 2 (for $\zeta$ negative). Similar relationships are found from (ii) when the ground state is $p_x$. No. 29 is plotted on this basis in figure 1(b). The rectangular hyperbolic form of these relations is well illustrated in this figure.

## References

[1] Krasnobaev A A, Votyakov S L and Krochalev V Ya 1988 *Spektroskopya Tsirconov, Svoistva, Geologicheskie Prilozheniya* (Moscow: Nauka)
[2] Claridge R F C, Mackle K M, Sutton G L A and Tennant W C 1994 *J. Phys.: Condens. Matter* **6** 3429–36
[3] Wyckoff R W C 1965 *Crystal Structure* vol 3 (New York: Wiley) pp 157–9
[4] Claridge R F C, Lees N S, Tennant W C and Walsby C J 1999 *J. Phys.: Condens. Matter* **11** 3571–80
[5] Barker P R and Hutton D R 1973 *Phys. Status Solidi* b **60** K109–K111
[6] Claridge R F C, Sutton G L A and Tennant W C 1997 *J. Magn. Reson.* **125** 107–13
[7] Claridge R F C, Tennant W C, Schweizer S and Spaeth J-M 1999 *J. Phys.: Condens. Matter* **11** 8579–89
[8] Walsby C J, Lees N S, Tennant W C and Claridge R F C 2000 *J. Phys.: Condens. Matter* **12** 1441–50
[9] Claridge R F C, Mackle K M, Sutton G L A and Tennant W C 1994 *J. Phys.: Condens. Matter* **6** 10 415–22
[10] Griffiths J H E, Owen J and Ward I M *Nature* **173** 439–41
[11] Nuttall R H D and Weil J A 1981 *Can. J. Phys.* **59** 1696–708

[12] Stapelbroek M, Bartram R H, Gilliam O R and Madacsi D P 1976 *Phys. Rev.* B **13** 1960–6

[13] Stapelbroek M, Gilliam O R and Bartram R H 1977 *Phys. Rev.* B **16** 37–43

[14] Barklie R C, Niklas J R, Spaeth, J-M and Bartram R H 1983 *J. Phys. C: Solid State Phys.* **16** 579–90

[15] Danby R J and Hutton D R 1980 *Phys. Status Solidi* **98** K125–K128

[16] Chase A B and Osmer J A 1966 *J. Electrochem. Soc.* **113** 198–9

[17] Claridge R F C, McGavin D G and Tennant W C 1995 *J. Phys.: Condens. Matter* **7** 9049–60

[18] Weil J A, Buch T and Clapp J E 1973 *Adv. Magn. Reson.* **6** 183–257

[19] Mombourquette M J, Weil J A and McGavin D G 1996 *Computer Program EPRNMR* University of Saskatchewan

[20] Vanotti L E and Morton J R 1968 *Phys. Rev.* **178** 448–53

[21] Bartram R H, Swenberg C E and Fournier J T 1965 *Phys. Rev.* A **139** 941–51

[22] Morton J R and Preston K F 1973 *J. Magn. Reson.* **30** 577–82

[23] Stoneham A M 1966 *Proc. Phys. Soc.* **89** 909–21

[24] Vinokurov V M, Gainullina N M, Evgrafova L A, Nizamutinov N M and Suslina A N 1971 *Sov. Phys.–Crystallogr.* **16** 262–5

[25] Solntsev V P and Shcherbakova M Ya 1972 *Dokl. Akad. SSSR* **1** 156–8